15ÈMES JOURNÉES DE L'HYDRODYNAMIQUE
22 - 24 novembre 2016 - Brest

Accurate characterisation of nearshore hydrodynamics for marine renewable energy applications

Caractérisation fine de l'hydrodynamique en zone littorale pour des applications en énergies marines renouvelables

A. Varing [a*], J.F. Filipot [a], V. Roeber [b], R. Duarte [a]
[a] France Energies Marines, 15 rue Johannes Kepler, Technopole Brest Iroise, 29200 Brest, France
[b] International Research Institute of Disaster Science, Tohoku University 468-1-E304 AzaAoba, Aramaki, Aoba-ku, Sendai 980-0845, Japan

Abstract

Numerical simulations of waves propagating over the potential wave energy site of Esquibien are performed with a phase-resolving model. The Boussinesq Ocean and Surf Zone model, BOSZ, is selected and its applicability for wave transformation is validated with observations. BOSZ accounts for the dominant processes that affect nearshore zone such as refraction, diffraction, reflection, wave breaking and nonlinear interaction. Predicted evolution of the spectral shape agrees well with the observations. Since BOSZ is a phase-resolving model, it is able to capture nonlinear energy transfers to super-harmonics and sub-harmonics. In the present simulation, BOSZ is efficient at capturing the infragravity (IG) peak frequency but overestimates the amount of IG wave energy which is gained by nonlinear interactions in the shoaling region. Since significant errors are observed close to the input wave boundary, a more realistic frequency-directional spectrum is required to improve the simulation.

Résumé

Des simulations numériques de vagues se propageant sur le potentiel site houlomoteur d'Esquibien sont réalisées avec un modèle à phase résolue. Le modèle BOSZ (Boussinesq Ocean and Surf Zone) est sélectionné et son utilisation est validée à partir d'observations. BOSZ tient compte des processus dominants affectant les zones littorales tels que la réfraction, la diffraction, la réflexion, le déferlement des vagues et les interactions non-linéaires. L'évolution des spectres simulés est cohérent avec les observations. BOSZ étant un modèle à phase résolue, il est en mesure de capturer les transferts d'énergie non linéaires vers les super-harmoniques et les sous-harmoniques. Dans la présente étude, le fréquence du pic d'onde infragravitaire est correctement estimée par BOSZ, mais le modèle surestime la quantité d'énergie de ces ondes longues qui est acquise par des interactions non linéaires dans la zone de shoaling. Des erreurs significatives étant observées à la frontière entrante, un spectre en fréquences-directions plus réaliste est nécessaire pour améliorer la simulation.

*Corresponding author. E-mail address : audrey.varing@gmail.com (A. Varing).

1 Introduction

Marine renewable energy (MRE) represents a huge potential for providing electricity worldwide. MRE devices are likely to be installed in nearshore waters for ease of access. Although progress is underway, there are still key challenges to be met in the development of MRE technology. The first challenge identified by Mueller and Wallace (2008) is to understand the resource in order to provide better ressource analysis. The capability to quantify the complex wave conditions is also essential to engineering design and to manufacturability, installation, operation, maintenance and survivability of wave energy devices. Shallow water energy resource is much more complex than that in deep water. Shallow water waves are modified by bottom topography and subject to physical processes such as shoaling, refraction, diffraction, nonlinear interactions, breaking and bottom friction. Many efforts have been made to incorporate this knowledge in numerical wave models. While models provide accurate description of large-scale wave patterns, most modeling difficulties remain in the nearshore areas (Mueller and Wallace, 2008). Different types of wave model exist with their advantages and drawbacks. Battjes (1994) classified the numerical models into phase-averaged and phase-resolving models.

The phase-averaged method has been widely used in the literature for modeling waves generated by the wind on large areas. A spectral model is a description of statistical properties of the sea surface (Cavaleri, 2006). This class of model computes the evolution of wave energy spectra while the phases are assumed to be random. The processes of wind generation, refraction and shoaling due to varying depth, energy dissipation due to bottom friction and depth-induced wave breaking are usually taken into account in these spectral models (Folley et al., 2010). Present phase-averaged wave models generally provide accurate results for large areas in deep and intermediate water depths. Because they loose the phase information, these models can not provide reliable results in nearshore areas (Rusu and Soares, 2012). Therefore there is a need for other modeling approaches that are accurate in shallow water for MRE applications.

An alternative approach to model the sea surface is the use of phase-resolving models. They describe the sea surface as a function of time over small areas. Their main limitations concern their operational use as they are computationally very demanding. They are also more sensitive to numerical instabilities (Rusu and Soares, 2012). Different phase-resolving wave propagation models have been developed during the last two decades such as the mild-slope equation and Boussinesq-type equations (Liu and Losada, 2002). They are often preferred because of their ability to accurately calculate diffraction, shoaling, refractions and nonlinearity. Focus is given here to Boussinesq-type models.

Numerical models based on Boussinesq-type formulation have proved their usefulness to accurately represent nearshore processes (Rusu and Soares, 2012). Boussinesq-type models aspire to resolve both wave-by-wave dynamics to reliably predict relevant nearshore processes and the dissipation associated with wave breaking. The standard Boussinesq-type equations for variable water depth were first derived by Peregrine (1967). Boussinesq-type equations take into account both nonlinear and frequency-dispersive features of wave motion, well representing wave propagation, but they are not automatically suited to model wave breaking, swash motion and wave overtopping. Nwogu (1993) improved the linear dispersion properties of the standard Boussinesq-type equations by using the velocity at an arbitrary distance from the still-water level as the velocity variable. These extended Boussinesq-type equations represent a practical tool to simulate the nonlinear transformation of irregular, multidirectional waves in water of varying depth prior to wave breaking. Because dissipation due to wave breaking is an important modeling issue, researchers have developed semi-empirical approaches to account for wave breaking in Boussinesq-type models (Wei et al., 1995; Madsen et al., 1997; Kennedy et al., 2000).

The objective of the present work is to implement in the Brittany French nearshore, high-resolution computational tools that are able to properly assess the nearshore processes occurring in the vicinity of a breakwater. The Esquibien breakwater area has been identified as a potential site for MRE by the French research program EMACOP (EMACOP, 2013). Esquibien bay has a challenging environment with waves approaching from the Atlantic ocean. Irregular wave trains coming from the deep water ocean are transformed during their propagation towards the shallow water at the coast. This involves complicated nonlinear processes such as triad interactions in relatively short distances. It is crucial to provide details of the wave evolution processes at this location to produce accurate input data useful for wave ressource assessment. An incorrect wave ressource assessment could induce wrong estimation of

wave farm profitability and not optimal MRE system design. A phase-averaged model does not model enough physical processes to accurately assess the wave transformations around the breakwater. In the present study, the Boussinesq Ocean and Surf Zone model BOSZ is used in two horizontal dimensions to capture nearshore processes around Esquibien breakwater. The objectives of the study are first to estimate BOSZ capacity by comparing modeled and observed data and then study nearshore physical processes and explore the model limits.

A short description of the Boussinesq-type model BOSZ is provided in section 2. Section 3 describes the Esquibien site, the observations data sets and the model setup. The model results are presented and discussed in section 4. To conclude the paper, the main findings are summarized in section 5.

2 BOSZ model

The Boussinesq Ocean and Surf Zone model, BOSZ, developped by Roeber (2010) include re-formulated depth-integrated equations from Nwogu's Boussinesq-type equations with conserved variables to handle nearshore processes in the subcritical as well as the supercritical regime. The model takes into account wave breaking through momentum conservation with energy dissipation based on an eddy viscosity concept. From a computational point of view, a Godunov-type scheme based on a Riemann solver integrates the evolution variables in time. Details of the numerical formulation can be found in Roeber (2010), Roeber et al. (2010) and Roeber and Cheung (2012).

BOSZ was originally applied to energetic waves in a fringing reef environment. Roeber and Cheung (2012) provide comprehensive validation of BOSZ with laboratory and field data corresponding to both continental and tropical island conditions. Another example of application to continental conditions is given in Filipot et al. (2013). In the Iroise Sea, this model is able to capture the main hydrodynamic processes such as refraction, shoaling, and wave breaking, but also second-order processes such as wave setup and the inherent recirculation in the surf zone. BOSZ has also proven to be a stable and accurate model for irregular bathymetry locations and extreme wave conditions. Predictions of storm-induced coastal flood hazards were performed by Li et al. (2014) who combined BOSZ to a phase-averaged model. Li et al. (2014) used BOSZ instead of SWAN for wave-by-wave simulation of surf and swash-zone processes. The phase-resolving approach of BOSZ involving a shock-capturing Boussinesq model better reproduces the wave conditions at the shore of a tropical island. This model could also be used in hazard assessment as explained by Roeber and Bricker (2015). Because BOSZ is a phase-resolving wave model resolving individual waves, it successfully captured destructive tsunami-like waves that struck a fringing-reef-protected town during a typhoon.

3 Site description, field campaign and model setup

The project site, Esquibien, is located on the north of Audierne bay, Brittany, France. It is an open coast exposed to south-west swells. Attention will be given to the wave transformation in front of the breakwater that has been identified as a potential wave energy site (Figure 1).

Field measurements are used to validate the model results. As part of the French national network of coastal *in-situ* measurements of waves CANDHIS, a Datawell directional wave buoy was installed in Audierne bay in December 2013 (CANDHIS, 2016). It was located 1.5 km offshore Esquibien breakwater at a depth of 16 m (Figure 2). The frequency spectrum of the wave buoy will be used to confront the modeled wave conditions from BOSZ close to the offshore boundary. Measurements of the wave field from pressure sensors were obtained in winter 2013-2014 in Esquibien bay as part of a field campaign undertaken during the French research project EMACOP and conducted by CEREMA and France Energies Marines. This project aimed at studying and promoting the development of marine energy systems in ports or coastal structures in France (Michard et al., 2015). Two OSSI pressure sensors positioned close to the breakwater are used in the present study (Figure 2). The pressure data were converted to free surface elevation using a linear transfert function. A wide range of conditions were encountered during the experiment. In this study, we chose to analyze measurements and simulations for relatively moderate wave conditions.

The BOSZ model is applicable to computational domains on the order of millions of cells. The present domain includes Esquibien bay as well as a portion of the open ocean. The selected rectangular

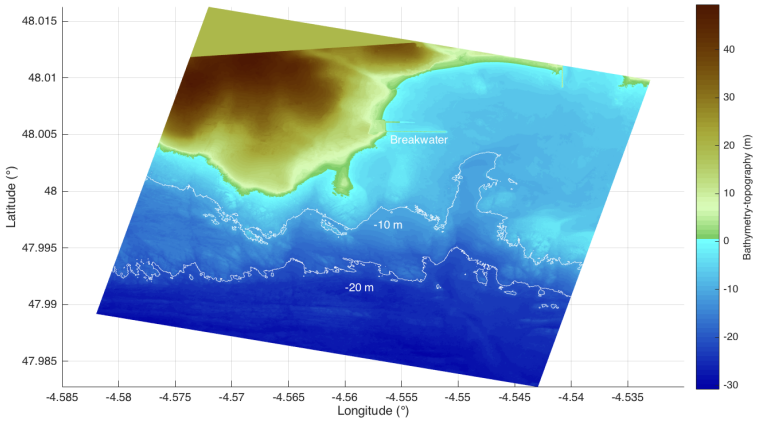

Figure 1 – Esquibien area

computational domain covers a region of 3000 m (long-shore, x-direction) by 3100 m (cross-shore, y-direction) visible on Figure 2. The spatial resolution is $\Delta x = 2.5$ m and $\Delta y = 1.25$ m. The bathymetry is extracted from the seamless digital terrain model LITTO3D (Pastol et al., 2007) and it is used without smoothing. The bottom roughness effect on the wave field is taken into account using a Manning coefficient of 0.025 for rock seabed. Individual waves are generated along the southern boundary by an internal wavemaker generating waves through a source function approach. For optimal performance, the domain has been rotated to find a compromise between shadow on the sides of the domain due to waves direction and having a uniformly flat bathymetry offshore. The water outside the 20 m contour is assumed to have a uniform depth of 20 m for a better implementation of the internal wavemaker. Sponge layers on all sides of the domain absorb the outgoing wave energy and act as open boundary conditions.

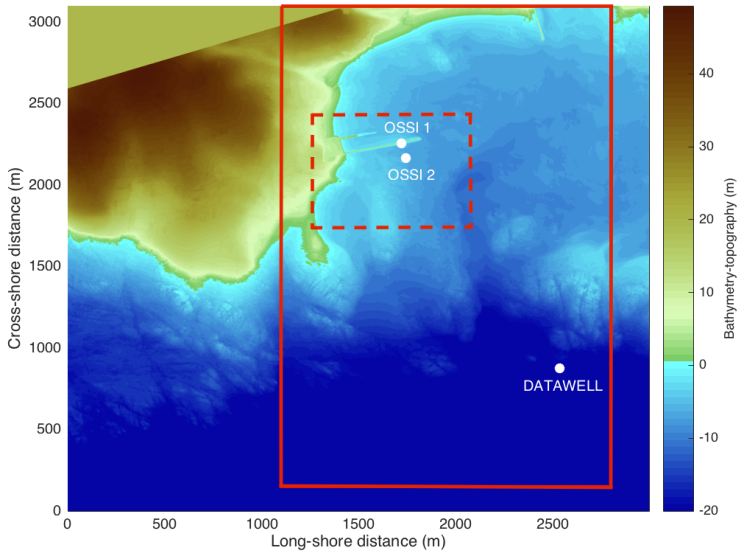

Figure 2 – Computational domain - The red solid line indicates the domain retained for result analysis and the red dotted line shows the breakwater domain.

In order to model realistic wave conditions to be compared with *in-situ* measurements, the hindcast model spectra of the regional model HOMERE (Boudière et al., 2013) are taken as input wave conditions. The closest point from HOMERE ($-4.566°$E, $47.984°$N) is situated at a few tens of meters from the offshore boundary. A moderate energetic event is modeled and analyzed in this study with a significant wave height (Hs) of 2.44 m, a peak period (Tp) of 14.1 s, a peak wave direction of 241°N associated to a spreading angle of 23.2°. The input frequency-direction spectrum is determined from a TMA frequency spectrum, which is a JONSWAP spectrum modified for shallow water, and a

normalized directional distribution symmetric about the direction of the peak direction. Simulations at mid-tide level will be discussed. Observations with a duration of 30 minutes around the mid-tide levels will be used to validate the model. We therefore expect few discrepancies between model results and observations data resulting from tide level changes.

The BOSZ model utilizes OpenMP for parallel processing within a computing node. In the present study, BOSZ was run on 4 processors. The domain requires approximately 1.5 hour for 1 minute of elapsed time. The numerical model uses a Courant number of 0.5 preventing the fastest wave from traversing more than one grid cell within a time step under breaking wave conditions (Roeber and Cheung, 2012). The total runtime of BOSZ is 1 hour to properly develop the offshore and nearshore sea state. The last 30 minutes of the simulations will be used for results analysis.

4 Results and discussion

Results are represented on a domain smaller than the computational domain because of a shadow on the left of the domain and the sponge layers. The shadow does not affect the area of interest close to the breakwater. The exploited outputs from BOSZ simulations are the water surface elevation. The significant wave height is determined from the sea surface elevation during the computation at each mesh. Because of storage constraints, the full time series of sea surface elevation are stored for one mesh over thirty and also at the locations of the pressure sensors and the Datawell buoy. This allows to compute the wave power at a lower spatial resolution. Integral parameters and spectra of modeled and observed data are compared at the pressure sensors and Datawell locations in sections 4.2 and 4.3. From these comparisons, the accuracy of the model to represent different nearshore wave processes is explored. A focus on infragravity (IG) waves is realized (section 4.4).

4.1 Wave field description

The observation of the significant wave height on Figure 3c indicates that swell coming from 241°N is submitted to refraction because of the water depth variations. The water depth decreases rapidly in front of the breakwater and the orientation of the waves changes so that the wave crests line up with the breakwater (Figure 3d). As seen on Figures 3a and 3b, the wave crest lines of the surface elevation turn around the island and finally line up with the breakwater because of the bathymetry, as observed with the significant wave height figures.

With this swell direction the breakwater ends up mostly in the shadow of the island on the left of the domain. According to Figure 3d, the Hs in front of the breakwater is small compared to a few meters further east. Important wave height variations are visible in front of the breakwater. The incoming waves are submitted to reflection on the breakwater. From Figure 3b, it is easy to identify reflected wave crests and troughs crossing incident waves. In the vicinity of the breakwater, there are clear interferences between the incident and reflected waves creating standing waves characterized by nodes and anti-nodes.

In front of the breakwater, between $x = 1500$-1700 m and $y = 1700$-2000 m, there is an area where the Hs increases. This is a shoaling zone associated with a shoal zone visible on Figure 2. After this zone of shoaling, the Hs decreases rapidly, it is the breaking zone. There is a second more intense shoaling zone on the right of the domain close to the Datawell buoy with Hs of up to 3 m. This shoaling is also the consequence of an important decrease of the water depth.

To provide an insight of the wave energy ressource estimated from the model results, the wave power is calculated from equation 1 :

$$P = \rho g \int_0^\infty C_g(f) S(f) df \tag{1}$$

where ρ is the density of water, g is the acceleration due to gravity, C_g is the group velocity and $S(f)$ is the elevation variance obtained from a Fourier transform of the sea surface elevation time series. Because the domain is in shallow water, waves are non-dispersive and the group velocity is independent of the frequency and can be approximated as $C_g = \sqrt{gh}$. Figure 4 shows that most wave power is located offshore. At the breakwater, the wave power is less than 10 kW/m.

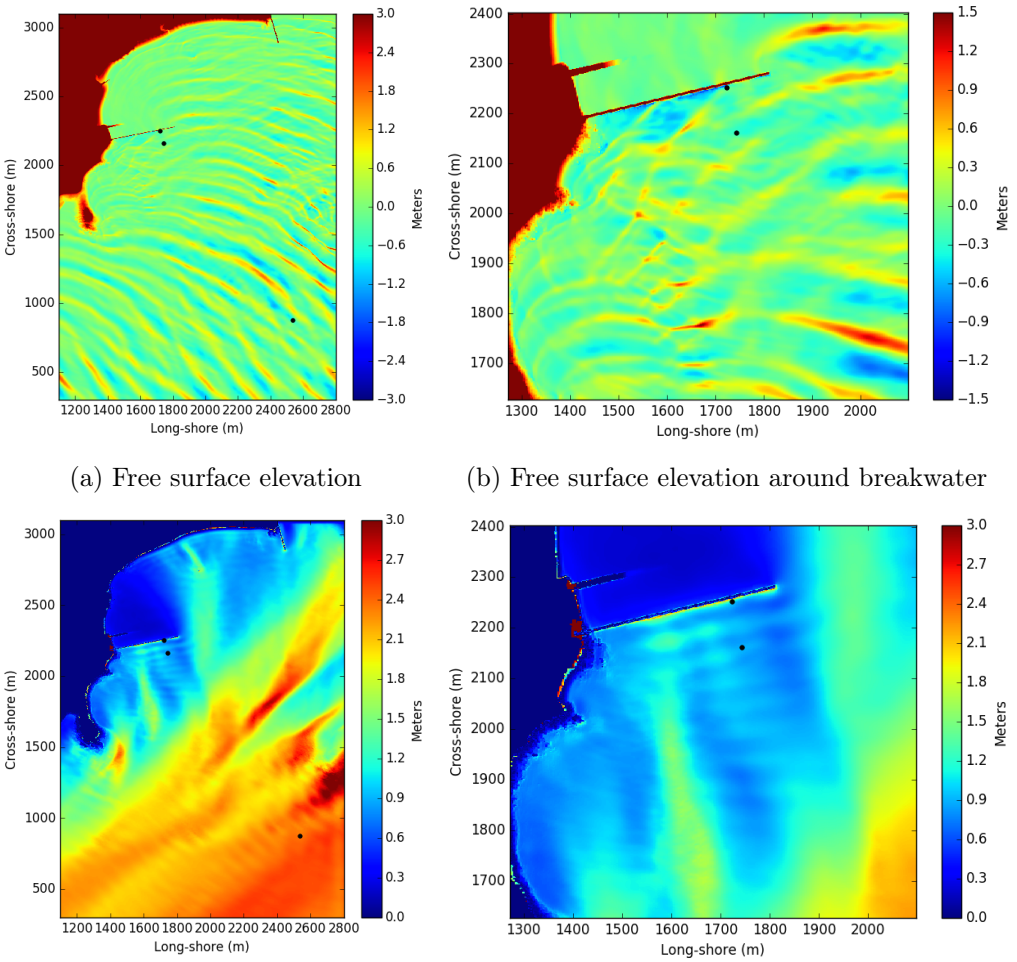

(a) Free surface elevation

(b) Free surface elevation around breakwater

(c) Significant wave height

(d) Significant wave height around breakwater

Figure 3 – Left panels present a global view and right panels present the wave field around the breakwater.

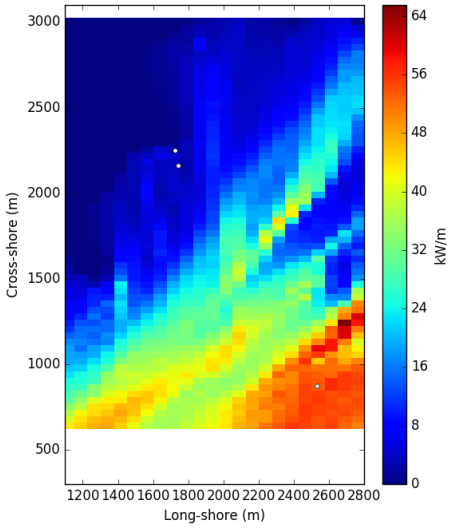

Figure 4 – Wave power

4.2 Integral wave parameters analysis

Further analysis is required to compare more precisely the model outputs and the observations. Hs and Tp are computed from the sea surface elevation time series at the three observations locations (the two pressure sensors and the Datawell buoy). BOSZ results are confronted to the observations in Table 1. Regarding Hs, more important errors are observed close to the offshore boundary and at the foot of the breakwater. Lower error is found at OSSI 2 with an 8% underestimation of Hs. Overall, the Hs mean error is 13.7%. The comparison between computed and observed Tp is good with errors lower than 10% at all locations.

	OSSI 1	Bosz	Er (%)	OSSI 2	Bosz	Er (%)	Datawell	Bosz	Er (%)
Hs (m)	1.32	1.09	17	0.95	0.86	8	2.11	2.45	16
Tp (s)	14.6	16.0	9	14.6	14.2	3	14.3	13.5	6

Table 1 – Integral parameters

4.3 Probability distribution and elevation spectra

To further investigate the discrepancy between the predicted and measured waves, the probability density function (pdf) of the free surface elevation (Figure 5) and the frequency spectra (Figure 6) are calculated at the sensors locations for both simulation and observations.

As seen on Figure 5, the pdf for all locations presents relatively good agreement between the predicted and measured data, although there are some differences. The red curve indicates the gaussian distribution. The observations seem to be more linear than the modeled waves. This might be due to the fact that the sea surface elevation has been calculated applying the linear theory to the pressure sensors data. This induces a loss of the nonlinear feature of the waves. The most important difference is visible at OSSI 1 where the model presents a lot of small waves. It is rather complex to model the dynamic at the foot of the breakwater since it is dominated by interferences between incident and reflected waves.

Figure 6 presents the spectral energy density of the observations and BOSZ simulation. The measured signal at the Datawell location is a typical sea-swell spectrum. At this location, close to the offshore boundary, the predicted spectrum agrees well with the observations, except for the higher harmonics. Whereas the Datawell buoy presents a very sharp spectrum without harmonics, BOSZ simulation indicates the presence of the first harmonic of the main peak frequency ($f_p = 0.07$ Hz). When the waves arrives at OSSI 2, they have undergone transformations because of refraction, shoaling and nonlinear energy transfers. BOSZ is able to represent the transfers of energy from the main peak frequency to both super-harmonics and sub-harmonics. Transfers of energy to higher harmonics are an indication that waves are becoming more nonlinear with sharper crests and flatter troughs. While higher harmonics are a bit underestimated by BOSZ, lower harmonics in the IG band (0.004-0.04 Hz) are highly overestimated. The long waves peak of energy in the IG band has a frequency of 0.011 Hz. The spectral energy density at the foot of the breakwater (OSSI 1) has two peaks. Between OSSI 1 and 2, BOSZ indicates that a significant part of the energy has been shifted toward the IG band by taking a lot of energy to the main peak.

Contrary to phase-averaged models, phase-resolving models have the advantage to take into account nonlinear transfers of energy and thus they can model IG motions. However, the most significant errors on the wave spectra are linked to these long waves. The following section proposes a study of the IG waves in order to understand the origin of the differences between the model and the observations.

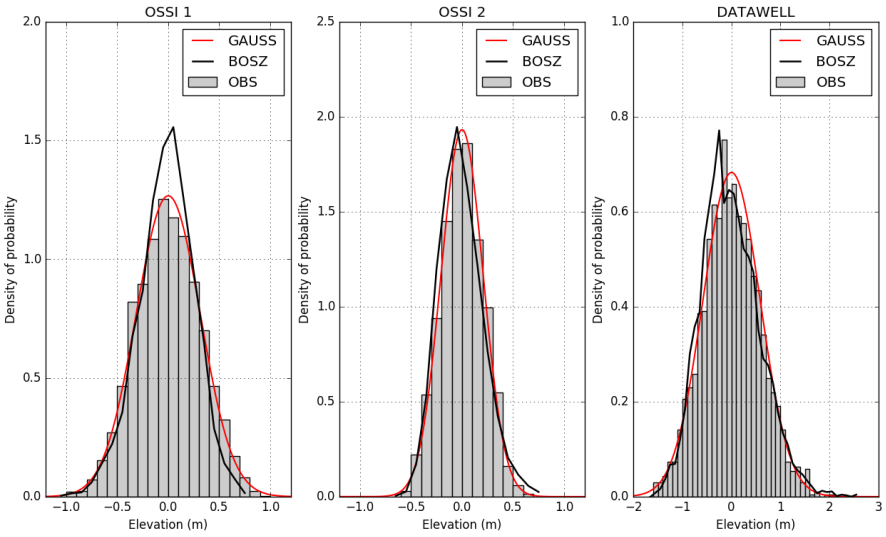

Figure 5 – Probability density function of free surface elevation

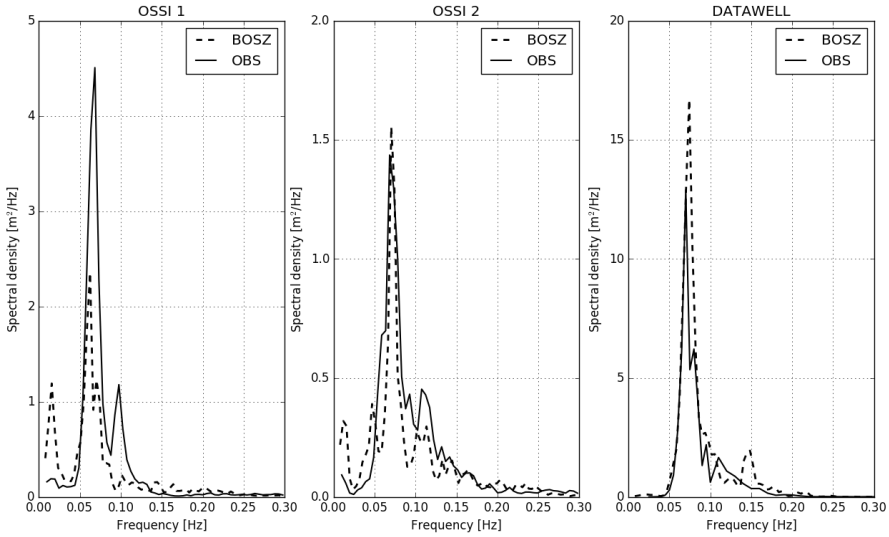

Figure 6 – Spectra determined from free surface elevation

4.4 Infragravity wave dynamics

IG waves are long period surface gravity waves which are important for harbor hydrodynamics, sediment transport, and other nearshore processes. A literature review is realized to explain the IG waves generation and dissipation processes.

4.4.1 Review of infragravity waves generation and dissipation mechanisms

IG waves have typical frequencies ranging from 0.004 Hz to 0.04 Hz (Herbers et al., 1995). Two mechanisms for the generation of IG waves have been identified.

Even if sea waves may look random, waves are organized into wave groups of sea-swell (SS) waves (frequency of 0.04-0.3 Hz) (Nakamura and Katoh, 1992). In deep water, nonlinear interactions between SS waves produce forced long waves in anti-phase with the wave group (Longuet-Higgins and Stewart, 1962). These long waves propagate at the same wave length and period as the SS wave groups and are known as bound IG waves. Their energy reaches its maximum amplitude before the group structure disappear due to SS waves breaking. Then the IG wave is not bound anymore and becomes a free wave (Herbers et al., 1995).

Another IG wave generation mechanism is the time-varying breakpoint based on a model of Symonds et al. (1982). Modulated groups of high and low SS waves amplitudes generate a time-varying breakpoint which induces a time-varying wave setup and hence shoreward and seaward directed free IG waves.

During their propagation, IG waves are submitted to dissipation. According to Henderson and Bowen (2002), IG waves can lose energy due to bottom friction. This mechanism would be dominant in flat and shallow regions such as coral reef where the friction coefficient is important (Pomeroy et al., 2012), but less significant on sloping beaches (Henderson et al., 2006; Van Dongeren et al., 2007). Once IG waves enter the surf zone, the wave motion becomes strongly nonlinear and energy is exchanged rapidly between SS and IG waves. Henderson et al. (2006) suggested the existence of nonlinear energy transfer back to SS frequencies through triad interactions in the inner surf zone. Closer to the shoreline, dissipation due to IG wave breaking could play a role (Battjes et al., 2004; Van Dongeren et al., 2007).

To explain model *versus* observations discrepancies in the IG band, a focus is made on IG generation and dissipation processes with the BOSZ model.

4.4.2 Infragravity waves in the model

From the model results, the objective of the present section is to confront both IG generation processes and identify if one of them (or both of them) is responsible for a too important IG waves generation in the model. Hs of IG waves is estimated by calculating the 0th-order of the spectral energy density in the frequency band from 0.004 to 0.04 Hz. Hs of IG waves is calculated over the domain with one mesh over thirty because of storage constraints (Figure 7). At the deepest water in the domain, close to the offshore boundary, IG energy is almost zero. The areas of highest significant IG wave height are the same as the areas of waves breaking (Figure 3c). IG waves seem to be generated during the process of SS waves breaking. Then they should have the same period as the SS wave groups as explained by Longuet-Higgins and Stewart (1962).

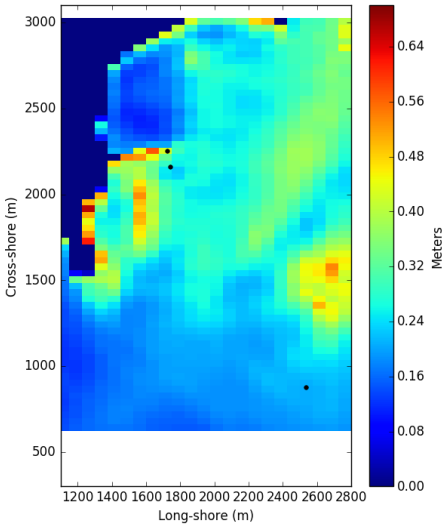

Figure 7 – Significant wave height of infragravity waves

The offshore structure of the waves group is then analyzed. The smoothed short-wave envelope is calculated from a Hilbert transform of the low pass filtered ($f < 0.1$ Hz) surface elevation data at the Datawell location (Sobey and Liang, 1986) (Figure 8). At this location it is possible to compare the modeled and observed group structures. Groups obtained from the simulations are more modulated than the observed groups. Their periods are irregular with both very small and very long groups. Some groups are dispersed and dominated by a few large waves. Even if there are strong differences in the distribution of the wave groups, the averaged group frequency is identical : 0.011 Hz. As explained in section 4.3, Figure 6 indicates that the peak frequency in the IG band for OSSI 1 and 2

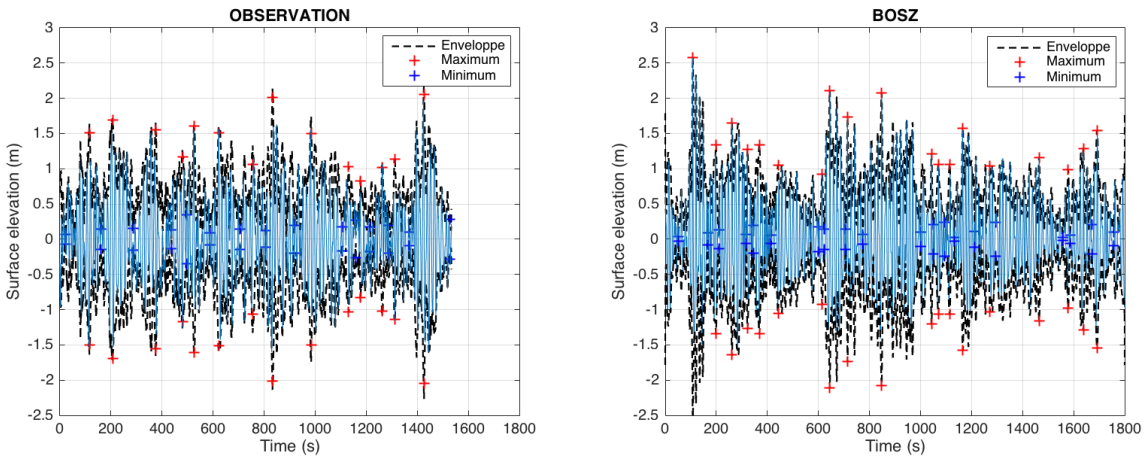

Figure 8 – Group structure at the Datawell location

is 0.011 Hz. From this, it is inferred that the offshore groups of SS waves generate IG waves at the same frequency as the wave groups in the shallow water close to the breakwater following Longuet-Higgins and Stewart (1962) study. Esquibien location presents a rather gentle slope, then according to Battjes et al. (2004), the released of bound long waves should be dominant. However, the possible reason for the overestimation of IG waves by the model could come from the second mechanism of IG waves generation identified by Symonds et al. (1982). Modeled groups are not as regular as in the observations, they have much smaller and higher amplitudes. This difference induce a time varying break point more important than in the observations. This has the effect of generating a varying wave setup and thus creating long waves. It is inferred from this that IG waves can be generated in the wave breaking process of wave groups because of a time-varying breakpoint. These free long waves can radiate away from the breakpoint, in both shoreward and seaward directions. This agrees with the theory of Symonds et al. (1982).

Because the Datawell location is close to the input boundary, there is no reason to observe such differences in the group structure unless the input spectrum does not correspond to the actual offshore wave conditions. The input spectrum might not be sufficiently accurate for the nearshore study performed here and lead to significant errors at low-frequency motions.

The previous section demonstrated the reason why IG waves could be overestimated by the model. An additional explanation could be that the model underestimates the dissipation of IG waves. Therefore, the different mechanisms of IG waves dissipation are discussed regarding the model results. A sensitivity analysis to bottom friction has been investigated with the BOSZ model. Since no difference was observed on the sea surface elevation and on the spectral energy density with the results presented in this paper (Manning coefficient of 0.025), the results are not shown. In the present configuration, bottom friction has no effect on the dissipation of IG waves, confirming the observations of Henderson et al. (2006) and Van Dongeren et al. (2007) on a sloping beach. Nonlinear energy transfer have also been analyzed by calculating the bispectra of the sea surface elevation following Herbers et al. (2000) and Péquignet et al. (2014). From these analysis it is not conclusive whether IG frequencies are transferred back to SS frequencies which would be a cause of IG wave dissipation. Finally, it is supposed that dissipation of the IG waves occurring in the model might be due to IG wave breaking at the breakwater. An extended array of sensors would be required to perform further analysis on dissipation of IG waves.

5 Conclusion and perspectives

In this study, the capabilities of BOSZ, a Boussinesq-type phase-resolving wave model, in simulating the waves transformation over the nearshore area of Esquibien bay have been performed. The applicability of BOSZ model has been investigated by comparison with observations. Model results show that the wave field is reasonably well reproduced. BOSZ generally produces a 13.7% error of significant

wave height for input wave conditions determined by a theoretical spectrum. Predicted evolution of the spectral shape agreed well with observations except at the IG frequency band. BOSZ is able to capture the IG peak frequency but highly overestimates the amount of IG wave energy. IG wave energy is gained by nonlinear interactions in the shoaling region. The overestimation of IG waves is attributed to a too important generation of free IG waves because of the time-varying breakpoint mechanism caused by irregular group structures. An accurate simulation of the short waves is required to represent waves group correctly. A more realistic frequency-directional spectrum is required to produce better results from the BOSZ model.

Future work could involve extending the BOSZ model validation with further spatial resolution analysis, wave conditions, still water levels as tidal range is quite large in the Esquibien area. For future investigation of IG waves, extended array of sensors measuring low frequencies could bring a lot of new information to quantify the magnitude of incoming and outgoing IG wave components to be compared with BOSZ simulations.

Acknowlegement

This work was made possible by the help of CEREMA and CETMEF which provided the pressure sensors data and Datawell buoy data respectively. I also would like to thank PREVIMER for supplying the model data (PREVIMER and HOMERE).

References

Battjes, J. (1994). Shallow water wave modelling. In *Int. Symp. on Waves - Physical and Numerical Modelling*, pages 1–23.

Battjes, J., Bakkenes, H., Janssen, T., and Van Dongeren, A. (2004). Shoaling of subharmonic gravity waves. *Journal of Geophysical Research: Oceans*, 109(C2).

Boudière, E., Maisondieu, C., Ardhuin, F., Accensi, M., Pineau-Guillou, L., and Lepesqueur, J. (2013). A suitable metocean hindcast database for the design of marine energy converters. *International Journal of Marine Energy*, 3.

CANDHIS (2016). Centre d'archivage national de données de houle in situ, `http://candhis.cetmef.developpement-durable.gouv.fr` (accessed : 2016-08-18).

Cavaleri, L. (2006). Wave modeling: Where to go in the future. *Bulletin of the American Meteorological Society*, 87(2):207.

De Bakker, A., Tissier, M., and Ruessink, B. (2014). Shoreline dissipation of infragravity waves. *Continental Shelf Research*, 72:73–82.

Elgar, S. and Guza, R. (1985). Observations of bispectra of shoaling surface gravity waves. *Journal of Fluid Mechanics*, 161:425–448.

EMACOP (2013). Projet national emacop, energie marines, côtières et portuaires, `http://www.emacop.fr` (accessed : 2016-08-18).

Filipot, J.-F., Roeber, V., Boutet, M., Ody, C., Lathuiliere, C., Louazel, S., Schmitt, T., Ardhuin, F., Lusven, A., Outré, M., et al. (2013). Nearshore wave processes in the iroise sea: field measurements and modelling. In *Coastal Dynamics 2013-7th International Conference on Coastal Dynamics*, pages p–605.

Folley, M., Elsaesser, B., and Whittaker, T. (2010). Analysis of the wave energy resource at the european marine energy centre.

Henderson, S. M. and Bowen, A. (2002). Observations of surf beat forcing and dissipation. *Journal of Geophysical Research: Oceans*, 107(C11).

Henderson, S. M., Guza, R., Elgar, S., Herbers, T., and Bowen, A. (2006). Nonlinear generation and loss of infragravity wave energy. *Journal of Geophysical Research: Oceans*, 111(C12).

Herbers, T., Elgar, S., and Guza, R. (1995). Generation and propagation of infragravity waves. *Journal of Geophysical Research: Oceans*, 100(C12):24863–24872.

Herbers, T., Russnogle, N., and Elgar, S. (2000). Spectral energy balance of breaking waves within the surf zone. *Journal of physical oceanography*, 30(11):2723–2737.

Hughes, S. A. (1984). The tma shallow-water spectrum description and applications. Technical report, DTIC Document.

Kennedy, A. B., Chen, Q., Kirby, J. T., and Dalrymple, R. A. (2000). Boussinesq modeling of wave transformation, breaking, and runup. i: 1d. *Journal of waterway, port, coastal, and ocean engineering*, 126(1):39–47.

Li, N., Roeber, V., Yamazaki, Y., Heitmann, T. W., Bai, Y., and Cheung, K. F. (2014). Integration of coastal inundation modeling from storm tides to individual waves. *Ocean Modelling*, 83:26–42.

Liu, P. L.-F. and Losada, I. J. (2002). Wave propagation modeling in coastal engineering. *Journal of Hydraulic Research*, 40(3):229–240.

Longuet-Higgins, M., Cartwright, D. E., and Smith, N. D. (1963). Observations of the directional spectrum of sea waves using the motions of a floating buoy. In *Ocean Wave Spectra, proceedings of a conference*, pages 111–136.

Longuet-Higgins, M. S. (1984). Statistical properties of wave groups in a random sea state. *Philosophical Transactions of the Royal Society of London A: Mathematical, Physical and Engineering Sciences*, 312(1521):219–250.

Longuet-Higgins, M. S. and Stewart, R. (1962). Radiation stress and mass transport in gravity waves, with application to 'surf beats'. *Journal of Fluid Mechanics*, 13(04):481–504.

Madsen, P. A., Sørensen, O., and Schäffer, H. (1997). Surf zone dynamics simulated by a boussinesq type model. part i. model description and cross-shore motion of regular waves. *Coastal Engineering*, 32(4):255–287.

Michard, B., Cosquer, E., Mallégol, A., Coignard, J., Amis, G., Filipot, J.-F., Kpogo-Nuwoklo, K. A., Olagnon, M., Ropert, F., and Sergent, P. (2015). Emacop project: characterising the wave energy resources of hot spots in brittany for on-shore wec. In *Proceedings of the 11th European Wave and Tidal Energy Conference*.

Mueller, M. and Wallace, R. (2008). Enabling science and technology for marine renewable energy. *Energy Policy*, 36(12):4376–4382.

Nakamura, S. and Katoh, K. (1992). Generation of infragravity waves in breaking process of wave groups. *Coastal Engineering Proceedings*, 1(23).

Nwogu, O. (1993). Alternative form of boussinesq equations for nearshore wave propagation. *Journal of waterway, port, coastal, and ocean engineering*, 119(6):618–638.

Pastol, Y., Le Roux, C., and Louvart, L. (2007). Litto d-a seamless digital terrain model. *The International hydrographic review*, 8(1).

Péquignet, A.-C. N., Becker, J. M., and Merrifield, M. A. (2014). Energy transfer between wind waves and low-frequency oscillations on a fringing reef, ipan, guam. *Journal of Geophysical Research: Oceans*, 119(10):6709–6724.

Peregrine, D. H. (1967). Long waves on a beach. *Journal of fluid mechanics*, 27(04):815–827.

Pomeroy, A., Lowe, R., Symonds, G., Van Dongeren, A., and Moore, C. (2012). The dynamics of infragravity wave transformation over a fringing reef. *Journal of Geophysical Research: Oceans*, 117(C11).

Roeber, V. (2010). *Boussinesq-type model for nearshore wave processes in fringing reef environment*. PhD thesis, Honolulu,University of Hawaii at Manoa,December 2010.

Roeber, V. and Bricker, J. D. (2015). Destructive tsunami-like wave generated by surf beat over a coral reef during typhoon haiyan. *Nature Communications*, 6.

Roeber, V. and Cheung, K. F. (2012). Boussinesq-type model for energetic breaking waves in fringing reef environments. *Coastal Engineering*, 70:1–20.

Roeber, V., Cheung, K. F., and Kobayashi, M. H. (2010). Shock-capturing boussinesq-type model for nearshore wave processes. *Coastal Engineering*, 57(4):407–423.

Roland, A. and Ardhuin, F. (2014). On the developments of spectral wave models: numerics and parameterizations for the coastal ocean. *Ocean Dynamics*, 64(6):833–846.

Rusu, E. and Soares, C. G. (2012). Modeling waves in open coastal areas and harbors with phase-resolving and phase-averaged models. *Journal of Coastal Research*, 29(6):1309–1325.

Schäffer, H. A., Madsen, P. A., and Deigaard, R. (1993). A boussinesq model for waves breaking in shallow water. *Coastal Engineering*, 20(3-4):185–202.

Sheremet, A., Guza, R., Elgar, S., and Herbers, T. (2002). Observations of nearshore infragravity waves: Seaward and shoreward propagating components. *Journal of Geophysical Research: Oceans*, 107(C8).

Sobey, R. J. and Liang, H.-B. (1986). Complex envelope identification of wave groups. In *Proc. 20th Int. Conf. Coastal Engng*, pages 752–766.

Symonds, G., Huntley, D. A., and Bowen, A. J. (1982). Two-dimensional surf beat: Long wave generation by a time-varying breakpoint. *Journal of Geophysical Research: Oceans*, 87(C1):492–498.

Thomson, J., Elgar, S., Raubenheimer, B., Herbers, T., and Guza, R. (2006). Tidal modulation of infragravity waves via nonlinear energy losses in the surfzone. *Geophysical Research Letters*, 33(5).

Van Dongeren, A., Battjes, J., Janssen, T., Van Noorloos, J., Steenhauer, K., Steenbergen, G., and Reniers, A. (2007). Shoaling and shoreline dissipation of low-frequency waves. *Journal of Geophysical Research: Oceans*, 112(C2).

Wei, G., Kirby, J. T., Grilli, S. T., Subramanya, R., et al. (1995). A fully nonlinear boussinesq model for surface waves. part 1. highly nonlinear unsteady waves. *Journal of Fluid Mechanics*, 294(7):71–92.